© (2014) Trans Tech Publications, Switzerland
doi:10.4028/www.scientific.net/AMM.465-466.1352

Verification of Fully Developed Flow Entering Diffuser and Particle Image Velocimetry Procedures

Normayati Nordin[1,a], Zainal Ambri Abdul Karim[2,b], Safiah Othman[1,c] and Vijay R. Raghavan[4,d]

[1]Faculty of Mechanical and Manufacturing Engineering, Universiti Tun Hussein Onn Malaysia, Parit Raja, 86400 Batu Pahat, Johor, Malaysia

[2]Department of Mechanical Engineering, Universiti Teknologi PETRONAS, Bandar Seri Iskandar, 31750 Tronoh, Perak, Malaysia

[4]OYL R&D Centre Sdn. Bhd., Taman Perindustrian Bukit Rahman Putra, 47000 Sungai Buloh, Selangor, Malaysia

[a]mayati@uthm.edu.my, [b]ambri@petronas.com.my, [c]safiah@uthm.edu.my, [d]vijay@oyl.com.my

Keywords: 3-D stereoscopic particle image velocimetry (PIV), diffuser, fully developed flow

Abstract. 3-D stereoscopic PIV is capable of measuring 3-dimensional velocity components. It involves a very sophisticated routine during setup, calibration, measurement and data processing phases. This paper aims to verify the 3-D stereoscopic PIV measurement procedures and to prove that the flow entering the diffuser is a fully developed flow. A diffuser inlet of rectangular cross-section, 130 mm x 50 mm is presently considered. For verification, the velocities from PIV are compared with the velocities from pitot static probe and theory. The mean velocity obtained using pitot static probe is 2.44 m/s, whereas using PIV is 2.46 m/s. It thus gives the discrepancy of 0.8%. There is also a good agreement between the mean velocity measured by PIV and theoretical value with the discrepancy of 1.2%. This minor discrepancy is mainly due to uncertainties in the experiments such as imperfect matching of coordinates between the probe and laser sheet, unsteadiness of flow, variation in density and less precision in calibration. Basically, the operating procedures of 3-D stereoscopic PIV have successfully been verified. Nevertheless, the flow entering diffuser is not perfectly developed due to the imperfect joining duct and the abrupt change of inlet cross-section introduced. Therefore, improvement to the existing rig is proposed by means of installing settling chamber with multiple screens arrangement and contraction cone.

Introduction

Particle image velocimetry (PIV) is a non-intrusive whole-field velocity measurement technique that has been used since the mid-1980s [1]. In contrast to other conventional methods such as hot wire anemometry and pitot static probe, PIV allows flows to be instantaneously interpreted both qualitatively and quantitatively. The application of PIV in research and industry is widespread, on account of its ease of use and accurate data representation. 3-D stereoscopic is the recently introduced PIV application, capable of measuring the third velocity component by means of correlating the 2-D PIV data. Involving a very sophisticated routine during setup, calibration, measurement and data processing, 3-D PIV demands proper judgement towards each procedure followed.

This study is a part of the work to investigate pressure recovery and flow uniformity in a 3-D turning diffuser [2]. The aims are to verify every procedure adopted in running 3-D stereoscopic PIV measurements and to prove that the flow entering the diffuser is fully developed. In the present work, a diffuser inlet of rectangular cross-section, 130 mm x 50 mm with five measurement points is considered. The hydrodynamic entrance length of $4.4D_hRe^{1/6}<L_{h,turb}<50D_h$ is introduced. The flow interpreted using 3-D PIV is compared with the flow calculated theoretically and the flow measured using pitot-static probe. The good results obtained with low associated uncertainties showed that the experimental practices were sound and well-run.

Literature Review

PIV Measurement Principles. Velocity vectors, $\bar{V}$ in PIV are derived from sub-sections (i.e. interrogation area, *IA*) of the target area of the particle-seeded flow by measuring the particle's displacement, Δx between two light pulses, Δt [3,4]. In this study, the target area of the flow is illuminated with double pulses Neodym: YAG laser. The laser light sheet thickness for stereoscopic PIV application is recommended to be approximately twice the size of the interrogation area (d_{IA}) projected out in object space [5]. In contrast to hot wire or pitot-static probe techniques, PIV measures the flow indirectly by determining the particle velocity instead of the flow velocity. Therefore, fluid mechanical properties of the tracer particle have to be examined in order to avoid significant discrepancies between fluid and particle motion. In air flows, smoke or oil drops within the diameter range of 0.5 µm to 10 µm are often used as tracer particles [1, 6].

Turbulence Characteristics. Many of conduits that are used are not circular in cross-section. Although the details of the flow in such conduits depend on the exact cross-sectional shape, many round pipe results can be carried over, with slight modification, to flow in conduits of other shapes. Practical, easy-to-use results can be obtained by introducing hydraulic diameter, $D_h=4A/P$. For turbulent flow such calculations are usually accurate to within about 15% [7, 8]. According to Elyasi [9], the most convenient way to compare the experimental results from PIV with the CFD simulation predictions is at a steady state condition with fully developed flow at the entrance of the test section. In order to generate such condition, several criteria should be made such as no flexible tube should be used, a precise blower control system should be required and systematic measurement procedures should be applied. Besides, the hydrodynamic length should be sufficiently introduced, $L_{h,turb}/D_h= 4.4Re^{1/6}$ [7], $L_{h,turb}/D_h= 1.359Re^{1/4}$ or $L_{h,turb} \approx 10D_h$ [8], $L_{h,turb} \approx 50\ D_h$ [9]. Turbulent flow along a wall can be considered to consist of four regions, namely viscous sublayer, buffer layer, overlap layer and outer turbulent layer [8]. Each layer is characterised by the distance from the wall, $r^+ = \frac{rU_*}{\upsilon}$, where u_* is a friction velocity that can be calculated using $u_* = \sqrt{\tau_w/\rho}$ and $r=b/2 - y$. Wall shear stress, τ_w can be determined using $\tau_w = \frac{1}{8} f \rho W_{avg}$, with friction factor, f that depends on Re and relative roughness, ε/D_h can be found from Moody chart. As the measurement points of P4 and P5 are located at $r^+>30$, they are both within the outer turbulent layer. Therefore, the one-seventh power-law velocity profile can be applied as following [8]:

$$\frac{W_{Pn}}{U_{\max}} = \left[1 - \frac{y}{R}\right]^{1/7} \tag{1}$$

where,
W_{Pn} = local velocity (m/s)
U_{max}= velocity at the centre point, i.e. W_{P2} (m/s)
y = measurement point from the centre (m)
$R = D_h/2$ (m)

Methodology

General Experimental Setup. Fig. 1(a) shows a schematic view of the experimental set up. The dimensions of duct are, a=130 mm width and b=50 mm height. The flow is considered incompressible with density, ρ= 1.164 kg/m^3 . Local air velocities at five points of measurement, as illustrated in Fig. 1(b), were measured using calibrated pitot static probe fitted to digital manometer of ±0.1 Pa resolution. Theoretical values were also calculated by means of the one seventh-power law velocity profile. These two methods of determining air velocities were then compared with PIV results for verification and validation purposes.

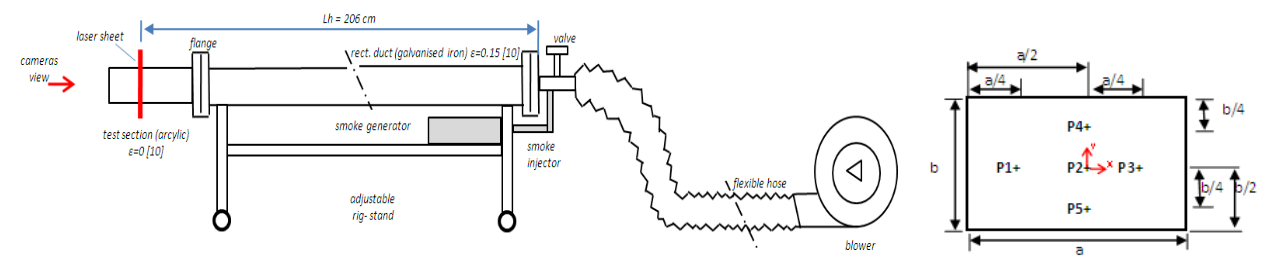

(a) (b)

Fig. 1. (a) Schematic diagram of the experimental setup (b) Local air velocities at five points of measurement; P1, P2, P3, P4 and P5

3-D Stereoscopic PIV Operation and Procedures. The principal dimensions of 3-D stereoscopic PIV measurement, which consists of the following sub-systems: (1) target flow of measurement; (2) calibration; (3) flow visualisation; (4) image detection and (5) data processing are introduced in Table 1.

Table 1. Principal dimensions of 3-D stereoscopic PIV measurement

Target flow of measurement	
Target flow	3-D air flow
Measurement facility	Diffuser inlet of rectangular cross-section connected to blower, 3-D PIV setup, Dynamic Studios software
Measurement plane	130 mm x 50 mm
Verification points	P1, P2, P3, P4 and P5
Calibration	
Magnification factor, *M*	0.1
Calibration target	Standard: dots 200 mm x 200 mm
Image Modeling Fit (IMF)	Pinhole
Number of images	5 images per cameras, each at different position of calibration target
Acquisition mode	Single frame mode
Flow visualisation	
Seeding particles	Eurolite smoke fluid 'P'
Average diameter, d_p	1μm [1]
Light source	Double pulse Nd:YAG laser
Wavelength	1064 nm, 532 nm
Pixel pitch	7.4 μm
Thickness of laser sheet	9.5 mm
Time between pulses, Δt	200 μs
Acquisition mode	Double frame mode
Image detection	
Camera	Two CCD cameras
Spatial resolution	1600 x 1200 pixels
Angle of cameras, θ	21^{o}
Data Processing	
Analysis	Cross correlation and 3D stereo method
Interrogation area (IA)	64 x 64 pixels

Results and Discussion

Pitot Static Probe and Theoretical Results as References. Considering the probe is perfectly installed and the average flow is steady, there are still uncertainties recorded. This is due to the significant fluctuations in the values of pressure and velocities, caused by the eddy motion in turbulent flow [8]. The inability to reset the system at exactly the same operating conditions from trial to trial also causes additional data scatter.

There were two main sources of errors; (1) the errors due to the variations of pressure and velocity ($s_{WPn,\ A}$) and; (2) the errors caused by the imperfect calibration of manometer ($b_{WPn,\ B}$). The uncertainty of pitot static probe measurement was contributed primarily by the source of error (1).

Table 2. Theoretical and pitot static probe results

Meas. point, P_n	Pitot static probe				Theo.
	Vel., $W_{Pn\text{-}pt}$ (m/s)	System. uncert., $b_{WPn,\,B}$ *	Rand. uncert., $s_{WPn,\,A}$ **	Stand. uncert., u_{WPn}	Vel., $W_{Pn\text{-}theo}$ (m/s)
P1	2.42	0.10	0.18	0.21	2.43
P2	2.43	0.10	0.18	0.21	2.43
P3	2.31	0.10	0.24	0.26	2.43
P4	2.58	0.10	0.10	0.14	2.28
P5	2.48	0.10	0.08	0.13	2.28
Mean	2.44	0.10	0.16	0.19	2.43

* *given by supplier,* ** *determined by means of statistical analysis*

Ideally, there is no significant variation of velocities at x-axis in the fully developed flow. Thus, W_{P1}, W_{P2} and W_{P3} are supposed to be the same. The flow varies at y-axis, W(y), with $W_{P4} = W_{P5}$ as both are symmetric. Since P4 is within outer turbulent layer, Eq. (1) can be applied to find W_{P4} by substituting W_{P2}= 2.43 m/s and W_{avg} =2.44 m/s. Table 2 presents the results of local air velocities associated with uncertainties measured using pitot static probe and theoretically calculated by means of one-seventh power law velocity profile. The mean velocity obtained by means of theoretical approach and pitot static probe were respectively W_{theo}=2.43 m/s and W_{pt}= 2.44 ±0.19 m/s. These results are used as reference points for verifying the PIV measurements.

Verification of 3-D Stereoscopic PIV Procedures. As depicted in Table 3 and 4, the range of velocity obtained using PIV is 2.31 – 2.91 m/s, whereas using probe and calculated theoretically they are 2.31 – 2.58 m/s and 2.28 – 2.43 m/s respectively. A major discrepancy of 17.3% and 27.6% is recorded for velocity at P5. This is mainly due to the imperfect matching of coordinates between the probe and laser sheet. However, there is still a good agreement between the mean velocity measured by PIV with the mean velocity measured by pitot static probe and calculated theoretically, with the discrepancy of 0.8% and 1.2% respectively. The procedures used are considered to be verified if the discrepancy is less than 10%.

Table 3. Comparison between PIV and pitot static probe velocity

Meas. point, P_n	PIV velocity, $W_{Pn\text{-}PIV}$ (m/s)	Press. probe velocity, $W_{Pn\text{-}pt}$ (m/s)	Discrepancy (%)
P1	2.31	2.42	4.5
P2	2.34	2.43	3.7
P3	2.26	2.31	2.2
P4	2.48	2.58	3.9
P5	2.91	2.48	17.3
Mean velocity (m/s)	2.46	2.44	0.8

Table 4. Comparison between PIV and theoretical velocity

Meas. point, P_n	PIV velocity, $W_{Pn\text{-}PIV}$ (m/s)	Theo. velocity, $W_{Pn\text{-}theo}$ (m/s)	Discrepancy (%)
P1	2.31	2.43	4.9
P2	2.34	2.43	3.7
P3	2.26	2.43	7.0
P4	2.48	2.28	8.9
P5	2.91	2.28	27.6
Mean velocity (m/s)	2.46	2.43	1.2

Verification of Fully Developed Flow Entering Diffuser. As shown in Fig. 2 the flow entering the diffuser is still not perfectly developed. This is due to the abrupt change introduced to the diffuser inlet from a small round pipe diameter to a rectangular duct cross-section and the imperfect joining of the duct. Therefore, several improvements to the existing test rig are proposed:

(1) Settling chamber with multiple screen arrangement and contraction cone is to be designed and fabricated, to damp all the disturbances and homogeneously distribute the flow.
(2) Flexible hose is to be avoided by levelling up the blower to the height of the PIV setup.
(3) A much stable blower that is controlled using three phase inverter is to be used.

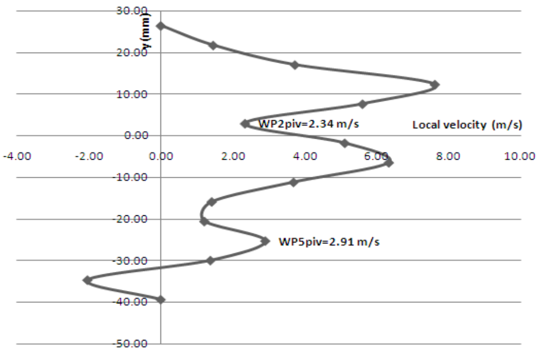

Fig. 2. Velocity profile at x= 0 cm

Conclusion and Recommendation

The procedures of operation for 3D stereoscopic PIV have successfully been verified and are justified to be used for future PIV measurement, considering the small average discrepancies of 0.8%-1.2% recorded. However, several improvements have to be made to the existing rig in order to promote a fully developed flow at the diffuser entrance.

Acknowledgements

This work was supported in part by the Fundamental Research Grant Scheme (FRGS) of the Ministry of Higher Education, Malaysia. The PIV work was conducted in the Aerodynamics Laboratory, Universiti Tun Hussein Onn Malaysia (UTHM).

References

[1] M. Raffel, C.Willert, S. Wereley and J. Kompenhans, Particle Image Velocimetry: A Practical Guide. 2nd ed. New York: Springer, 2007.
[2] N. Nordin, V.R. Raghavan and S. Othman, “Compatibility of 3-D turning diffusers by means of varying area ratios and outlet-inlet configurations,” ARPN Journal of Engineering and Applied Sciences, Vol. 7, No. 6, June 2012 (ISSN 1919-6608). Available: http://www.arpnjournals.com/jeas/volume_06_2012.htm
[3] Specialist Committee on Uncertainty Analysis, “Uncertainty analysis Particle Image Velocimetry,” *International Towing Tank Conference*, 2008.
[4] *Handbook of Particle Image* Velocimetry, Visualization Society of Japan, Moritika Publishing Co. Ltd., 2002.
[5] 3D Stereoscopic PIV Reference Manual, Dantec Dynamics, Skovlunde, Denmark, 2006.
[6] Dantec Dynamics. (2011, Oct. 29) Particle image velocimetry measurement principles [Online]. Available: http://www.dantecdynamics.com/Default.aspx?ID=820.
[7] D.F. Young, B.R. Munson, T.H. Okiishi and W.W. Huebsch, A Brief Introduction to Fluid Mechanics. 4rd ed. NJ: John Wiley & Sons, 2007.
[8] Y.A. Cengel and J.M. Cimbala, Fluid Mechanics; Fundamentals and Applications. 2rd ed. NY: McGraw Hill Higher Education, 2010.
[9] S. Elyasi, “Development of UV photo-reactor models for water treatment,” Ph.D Thesis, Faculty of Graduate Studies (Chemical and Biological Eng.), Univ. of British Columbia, Vancouver, 2009.